

## Numerical Investigation of Subcooled Boiling in a Vertical Pipe Using a Bubble-Induced Turbulence Model

**Mahmut D. MAT**

*Niğde University, Faculty of Engineering, Department of Mechanical Engineering,  
51100, Niğde-TURKEY*

**Kemal ALDAŞ**

*Niğde University, Aksaray Engineering Faculty, Department of Mechanical Engineering,  
68100 Aksaray-TURKEY*

*e-mail: kemalaldas@hotmail.com*

**Yüksel KAPLAN**

*Niğde University, Faculty of Engineering, Department of Mechanical Engineering,  
51100, Niğde-TURKEY*

Received 26.03.2001

### Abstract

A bubble-induced turbulence model is applied to subcooled boiling of water in a vertical pipe. The volume fractions, velocities, temperatures of water and steam and turbulence characteristics of the flow are estimated in a range of heat fluxes, subcooling temperatures and outlet pressures. The mathematical model involves solutions of transport equations for the variables of each phase with allowance for interphase transfer of momentum and energy. The numerical results agree satisfactorily with those of experimental and numerical results in the literature.

**Key words:** Subcooled boiling,  $k - \epsilon$  turbulence model, bubbles

### Introduction

Subcooled boiling occurs in many practical applications, such as in nuclear reactors, heat exchangers, steam generators and various power generation systems. Prediction of the void fraction profile, flow pattern and thermal field and velocity distribution is essential for design and safety analysis of such systems.

There is extensive research in the literature on the prediction of the void fraction in subcooled boiling. Most of these studies are based on empirical correlations due to the complex nature of the subcooled boiling process. Zuber *et al.* (1966) developed an expression for the axial void fraction considering the relative velocity between two phases. Using the model proposed by Zuber and Findlay (1965), Levy (1967) developed a formulation for the vapor volu-

metric fraction and tested the formulation with the experimental data in the literature. Kroger and Zuber (1968) developed an empirical formulation for the axial void fraction in a pipe depending on temperature, flow and local relative velocity. The formulation assumes prior knowledge of the location of incipient void formation. There are also a number of correlations available in the literature. The major drawback of these correlations is that they are valid only for the specific conditions in which they are tested. The more elaborate models consider basic transport equations governing the boiling and two-phase flow. Hu and Pan (1995) developed a mechanistic model derived from a one-dimensional two-phase model. However, the model was limited to only the axial direction and no information can be obtained in the radial direction. Zeitoun and Shoukri (1997) also developed a one-dimensional two-phase

model that accounts for interfacial mass and energy transport between two phases. However, this model also predicts the void fraction only in the axial direction and turbulence effects were not considered.

Lai and Farouk (1993) applied an advanced two-phase model to subcooled boiling flow in a pipe. This model was very useful for predicting the axial and radial void fraction profile, temperature distribution and velocity profile in the pipe. However, turbulence production due to the bubble motion was considered. It is evident from experimental measurements (Serizawa *et al.* (1986), Wang *et al.* (1987), Lopez de Bertodano *et al.* (1990)) that bubble motion affects the turbulence and therefore phase distribution. Theofanous and Sullivan (1982), and later Lance and Bataille (1991), experimentally found that at low liquid flow rates, grid generated turbulence can be linearly superimposed. However, at higher flow rates bubbles may have an adverse effect. Serizawa *et al.* (1986) and Wang *et al.* (1987) observed turbulence suppression at higher flow rates. Lopez de Bertodano *et al.* (1990) developed a  $k-\varepsilon$  turbulence model that accounts for turbulence production due to bubble motion. They applied this model to predict phase distribution in turbulent upward flow of bubble-water flow in a vertical pipe. They considered an isothermal problem with a prescribed void fraction at the inlet. Bubble production due to heating of a wall was not considered. The purpose of this study is to apply Lopez de Bertodano *et al.*'s (1994) model to estimate the void fraction, heat transfer and flow characteristic of subcooled boiling in a vertical pipe.

This paper is divided into four sections of which this introduction is the first. Section 2 contains the mathematical formulations and a summary of the numerical method. The computed results are presented in section 3. Section 4 contains the concluding remarks and summarizes the major findings of the study.

### Mathematical Modeling

Consideration is given to upward flow of water in a vertical pipe. The pipe height and diameter are 2 m and 0.024 m, respectively. The subcooled water enters the system at the bottom as shown in Fig. 1 and subsequently boils due to the constant heat flux supplied from the pipe walls. This system mirrors the experiment of Bartolemei and Chanturiya (1967) and the numerical study of Lai and Farouk (1993) for di-

rect comparison of the results. Only half of the pipe is considered due to the symmetry at the pipe axis.

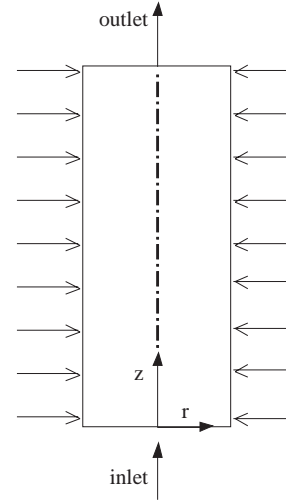


**Figure 1.** Schematic sketch of the system considered.

To represent the flow behavior and heat transfer in the system, a two-phase mixture of liquid and gas is considered. The phases are assumed to share space in proportion to their existence probabilities such that their volume fractions sum to unity in the flow field. This can be expressed mathematically as

$$\alpha_L + \alpha_G = 1 \quad (1)$$

where  $\alpha_L$  and  $\alpha_G$  are the volume fraction of liquid and gas respectively. The zone averaged quantities are obtained through the solution of separate transport equations for each phase.

Angular variation of the variables is assumed to be negligible in this problem and only radial and axial coordinates are considered. Within this framework, the governing equations for boiling two-phase flow can be expressed in cylindrical coordinates as follows:

#### Mass conservation

$$\frac{\partial}{\partial z} (\rho_i \alpha_i w_i) + \frac{1}{r} \frac{\partial}{\partial r} (r \rho_i \alpha_i v_i) = M_{i-int} \quad (2)$$

where subscripts i and j represent the phases and take the value of L and G in this problem. Subscripts L and G refer to liquid and gas phases, respectively, in this and subsequent formulations. The term on the right of the equation represents mass diffusion between two phases at the water-steam interface.

*Axial momentum (z direction)*

$$\begin{aligned} \frac{\partial}{\partial z} (\rho_i \alpha_i w_i^2) + \frac{1}{r} \frac{\partial}{\partial r} (r \rho_i \alpha_i w_i v_i) &= -\alpha_i \frac{\partial p}{\partial z} + \\ + F(w_j - w_i) + \frac{1}{r} \frac{\partial}{\partial r} (r \alpha_i \mu_{eff} \frac{\partial w_i}{\partial r}) + & \quad (3) \\ + \frac{\partial}{\partial z} (\alpha_i \mu_{eff} \frac{\partial w_i}{\partial z}) + F_b \end{aligned}$$

*Radial momentum (r direction)*

$$\begin{aligned} \frac{\partial}{\partial z} (\rho_i \alpha_i w_i v_i) + \frac{1}{r} \frac{\partial}{\partial r} (r \rho_i \alpha_i v_i^2) &= -\alpha_i \frac{\partial p}{\partial r} + \\ + F(v_j - v_i) + \frac{1}{r} \frac{\partial}{\partial r} (r \alpha_i \mu_{eff} \frac{\partial v_i}{\partial r}) + & \quad (4) \\ + \frac{\partial}{\partial z} (\alpha_i \mu_{eff} \frac{\partial v_i}{\partial z}) \end{aligned}$$

F in both momentum equations is the interface friction term and represents momentum exchange between the phases per unit volume, and  $F_b = \rho g$  is the buoyancy force g being the gravity vector.

*Energy equation*

$$\begin{aligned} \frac{\partial}{\partial z} (\rho_i \alpha_i w_i h_i) + \frac{1}{r} \frac{\partial}{\partial r} (r_i \rho_i \alpha_i v_i h_i) &= \\ \frac{1}{r} \frac{\partial}{\partial r} \left( r \alpha_i \frac{\mu_{eff}}{\text{Pr}_{eff}} \frac{\partial h_i}{\partial r} \right) + \frac{\partial}{\partial z} \left( \alpha_i \frac{\mu_{eff}}{\text{Pr}_{eff}} \frac{\partial h_i}{\partial z} \right) + S_{i-int} & \quad (5) \end{aligned}$$

where  $\text{Pr}_{eff}$  is the effective Prandtl number, which includes laminar and turbulent contributions, and  $S_{i-int}$  represents energy exchange between two phases at the interface.

*Auxiliary equations*

$M_{i-int}$  in equation (1) represents the mass transfer between two phases at the steam-water interface.  $M_{i-int}$  is computed from the heat transfer balance since evaporation and condensation occur at the interphase, thus

$$\begin{aligned} M_{G-int} = M_{L-int} = \\ \frac{\lambda_G A_{int} (T_G - T_{sat}) - \lambda_L A_{int} (T_L - T_{sat})}{\Delta H} \end{aligned} \quad (6)$$

where  $\lambda_L$  and  $\lambda_G$  are the heat transfer coefficients at the steam-water interphase.  $\lambda_L$  and  $\lambda_G$  are calculated from experimental data on heat transfer from spheres are valid over the entire Reynolds and Prandtl number range (Rosten and Spalding, 1986).

$\Delta H$  is the latent heat of vaporization or condensation at a given pressure.  $A_{int}$  is the interfacial area for unit volume and the calculated as

$$A_{int} = \frac{6\alpha}{d_b} \quad (7)$$

where  $d_b$  is the bubble diameter. A constant value of  $d_b=1\text{mm}$  is chosen (Lai and Farouk, 1993) in all the calculations presented in this study.

The interphase friction term, F, in momentum equations can be expressed as

$$F = 0.75 \frac{c_d \rho_1 \alpha_L \alpha_G}{d_b} |u_r| \quad (8)$$

where  $u_r$  is the slip velocity vector between two phases and  $c_d$  is the drag coefficient. There are extensive works on the drag coefficient in the literature. The ‘‘Dirty water’’ model of Kuo and Wallis (1988) is employed here. In this model,

$$c_d = \left\{ \begin{array}{ll} 6.3/Re_b^{0.385} & Re_b > 100, We \leq 8 \\ 2.67 & Re_b > 100, We > 8 \\ We/3.0 & Re_b > 2065.1/We^{2.6} \end{array} \right\} \quad (9)$$

where  $Re_b$  is the Reynolds number based on the gas bubble diameter,

$$Re_b = \frac{\rho_1 |u_r| d_b}{\mu_1} \quad (10)$$

and  $We$  is the Weber number defined as,

$$We = \frac{\rho_1 |u_r|^2 d_b}{\gamma} \quad (11)$$

where  $\gamma$  is the interfacial tension between the phases.

$S_{i-int}$  is the interphase heat transfer term can be expressed as,

$$S_{i-int} = \lambda_i A_{int} (T_i - T_{sat}) + \dot{M}_{i-int} (h_i - h_{sat}) \quad (12)$$

where  $\lambda_i$  is the heat transfer coefficient and  $M_{i-int}$  is the rate of mass transfer at the water-steam interface.

### Turbulence model

Flow under the conditions considered in this study is turbulent in all cases. It is crucial to choose a turbulence model that is suitable for this system. Therefore, a modified  $k - \varepsilon$  model that accounts for turbulence production due to bubble motion is employed here.

Effective viscosity includes both laminar and turbulent contribution in this problem, thus,

$$\mu_{eff} = \mu_t + \mu_l \quad (13)$$

Turbulent viscosity is calculated from a modified version of the  $k - \varepsilon$  model that accounts for turbulence induced by the bubble motions. Turbulent (eddy) viscosity is calculated from,

$$\mu_t = \frac{c_\mu \rho_1 k^2}{\varepsilon} \quad (14)$$

where  $c_\mu$  is an empirical constant and the parameters  $k$  and  $\varepsilon$  represent the turbulence production and dissipation mechanism.

The transport equations governing the  $k$  and  $\varepsilon$  terms are,

*k-equation*

$$\begin{aligned} \frac{\partial}{\partial z} (\rho_L \alpha_L w_L k) + \frac{1}{r} \frac{\partial}{\partial r} (r \rho_L \alpha_L v_L k) = \\ \frac{1}{r} \frac{\partial}{\partial r} (r \alpha_L \Gamma_L \frac{\partial k}{\partial r}) + S_k \end{aligned} \quad (15)$$

*$\varepsilon$  equation*

$$\begin{aligned} \frac{\partial}{\partial z} (\rho_L \alpha_L w_L \varepsilon) + \frac{1}{r} \frac{\partial}{\partial r} (r \rho_L \alpha_L v_L \varepsilon) = \\ \frac{1}{r} \frac{\partial}{\partial r} (r \alpha_L \Gamma_\varepsilon \frac{\partial \varepsilon}{\partial r}) + S_\varepsilon \end{aligned} \quad (16)$$

$\Gamma_k$  and  $\Gamma_\varepsilon$  are diffusion coefficients and expressed as

$$\Gamma_k = \mu_l + \frac{\mu_t}{\sigma_k} \quad (17)$$

$$\Gamma_\varepsilon = \mu_l + \frac{\mu_t}{\sigma_\varepsilon} \quad (18)$$

where  $\sigma_k$  and  $\sigma_\varepsilon$  are Schmidt numbers for  $k$  and  $\varepsilon$  respectively.  $S_k$  and  $S_\varepsilon$  are source terms and are given as

$$S_k = \rho r_L \alpha_L (G_k - \varepsilon) + \alpha_L G_{kb} \quad (19)$$

$$S_\varepsilon = \rho_L \alpha_L \frac{\varepsilon}{k} (C_L G_k - C_2 \varepsilon) + \alpha_L C_L G_{kb} \frac{\varepsilon}{k} \quad (20)$$

$G_k$  is the rate of production of turbulent energy and is expressed as

$$G_k = \mu_t \left\{ \left( \frac{\partial w_1}{\partial r} + \frac{\partial v_1}{\partial z} \right)^2 + 2 \left[ \left( \frac{\partial w_1}{\partial z} \right)^2 + \left( \frac{\partial v_1}{\partial r} \right)^2 \right] \right\} \quad (21)$$

The second terms in equations (19) and (20) are the turbulence production due to the motion of bubbles. Lopez de Bertodano [13] proposed following equations for  $G_{kb}$ :

$$G_{kb} = 0.75 \frac{c_b c_d \rho_1 \alpha_1 \alpha_2}{d_b} |u_r|^3 \quad (22)$$

The values of the constant employed in this study are given in Table 1.

**Table1.** The values of model constants used in computations

| $C_b$ | $C_p$ | $C_1$ | $C_2$ | $C_k$ | $C_\varepsilon$ |
|-------|-------|-------|-------|-------|-----------------|
| 0.04  | 0.09  | 1.44  | 1.92  | 1.0   | 1.3             |

### Boundary conditions

The numerical simulation exactly mirrors the experiment in Bartolemei and Chanturiya (1967) and the numerical study of Lai and Farouk (1993). The sub-cooled water enters the pipe and is heated from the wall along the pipe. The effects of heat flux and outlet pressure on the void fraction profile, temperature distribution and velocity field are examined. The cases considered are summarized in Table 2.

**Table 2.** Cases considered

| Case # | Inlet temp.<br>(°C) | Inlet<br>subcooling<br>(°C) | Outlet<br>pressure<br>(MPa) | Mass flux<br>kg/ms | Heat flux<br>kW/m <sup>2</sup> |
|--------|---------------------|-----------------------------|-----------------------------|--------------------|--------------------------------|
| Case 1 | 177.4               | 22.6                        | 1.5                         | 890                | 380                            |
| Case 2 | 149.1               | 50.9                        | 1.5                         | 890                | 790                            |
| Case 3 | 210                 | 25                          | 3                           | 890                | 380                            |
| Case 4 | 186.9               | 48.1                        | 3                           | 890                | 790                            |
| Case 5 | 231                 | 24                          | 4.5                         | 890                | 380                            |
| Case 6 | 205                 | 50                          | 4.5                         | 890                | 790                            |

The boundary wall is fixed and a log-law is employed to calculate the velocity component parallel to the wall. Following Launder and Spalding (1974),

$$\frac{u_1}{u_\tau} = \left(\frac{1}{\kappa}\right) \ln y^+ + 5.4 \quad (23)$$

where  $\kappa$  (=0.435) is the von-Karman constant,  $u_\tau$  is the shear velocity and  $y^+$  is the dimensionless distance of the node from the wall and is expressed as

$$y^+ = \frac{yu_\tau}{\mu_1} \quad (24)$$

$$u_\tau = \left(\frac{\tau_w}{\rho_1}\right)^{0.5} \quad (25)$$

where  $\tau_w$  is the wall shear stress.  $k$  and  $\varepsilon$  near the wall are calculated from the following relations (Launder and Spalding (1974)).

$$k = 4.2u_\tau^2 \quad (26)$$

$$\varepsilon = \frac{u_\tau^3}{\kappa y} \quad (27)$$

### Numerical method

The set of transport equations presented above is integrated over finite control volume and solved using the PHOENICS computer code (Rosten and Spalding, 1986). The code employs a fully implicit scheme that uses the IPSA algorithm (Singhal and Spalding, 1979). Only half the pipe is solved due to symmetry at the pipe axis. Ten grids in the radial direction and 50 grids in the axial direction are employed after a grid refinement test. A typical CPU time on a Pentium 200 PC was 20 minutes.

### Results

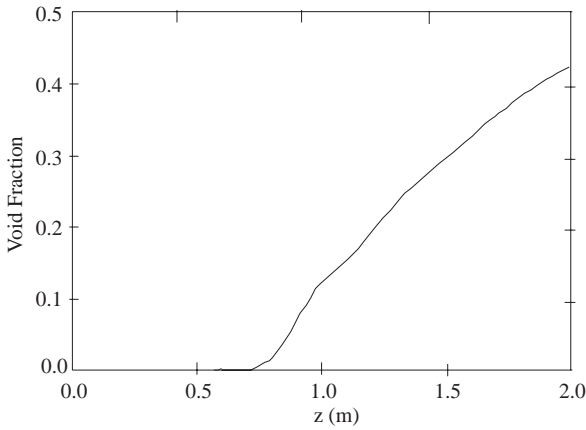
Boiling water may exhibit different flow patterns depending on the processing conditions and geometry. Here only heat transfer to subcooled water and bubbly boiling are considered.

Figure 2 shows the average void fraction distribution along the pipe axis. A general characteristic of the boiling is to transfer heat into continuous liquid phase up to around  $z=0.5$  m. After subcooled water reaches the saturation temperature, boiling is initiated. Boiling curve exhibits a parabolic increase after the onset of boiling. As shown in Fig. 3, boiling is concentrated near the heated wall for the flow regime considered here. It is seen that the void fraction is substantially higher adjacent to the wall and decreases towards the center.

Figure 4 shows the axial temperature profiles at three radial locations along the pipe. Temperature increases in the pipe due to the heating from the pipe wall and remains constant after the saturation temperature is reached. However, a slight superheating is evident adjacent to wall after the saturation temperature.

Radial temperature profiles at three locations are shown in Fig. 5. Thermal non-equilibrium is evident in this figure. There are large temperature differences between the center and wall of the pipe at  $z=0.5$  m, where bubble production starts close to wall while the center temperature is below the saturation temperature. Non-equilibrium conditions decrease along the pipe and a radially uniform temperature distribution is reached around  $z=1.5$  m. There is a slight superheating close to the wall.

Figure 6 shows the radial distribution of mean axial fluid velocity at three locations along the pipe.



**Figure 2.** Average void fraction distribution along the pipe axis (case 1).

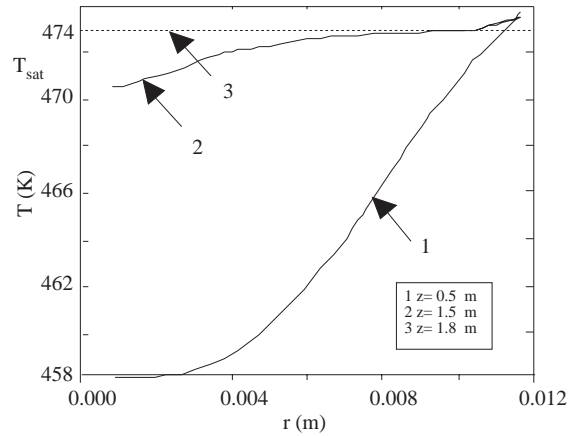


**Figure 5.** Estimated axial temperature profiles at three radial locations (case 1).

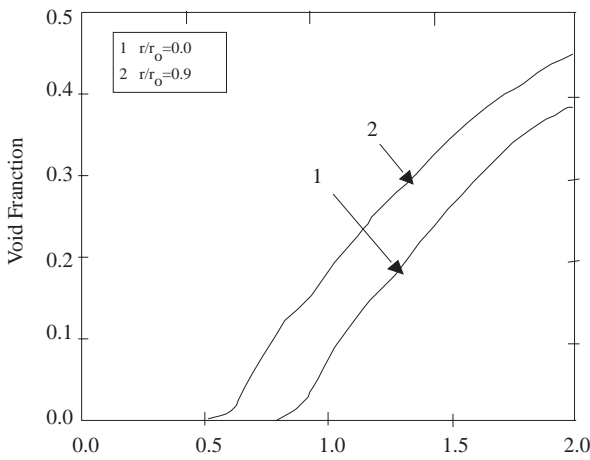


**Figure 3.** Axial void fraction distribution at two locations in the pipe (case 1).

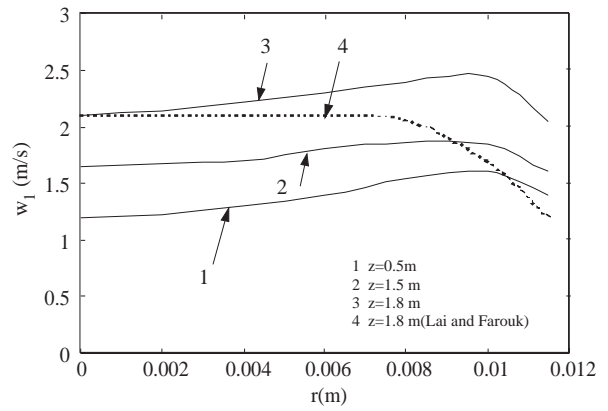


**Figure 6.** Radial distribution of axial liquid velocity at three locations along the pipe

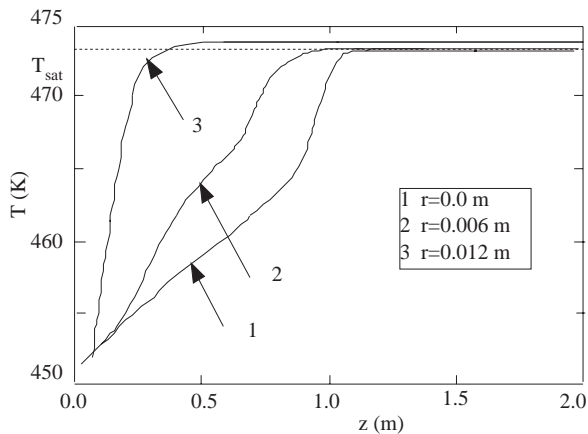
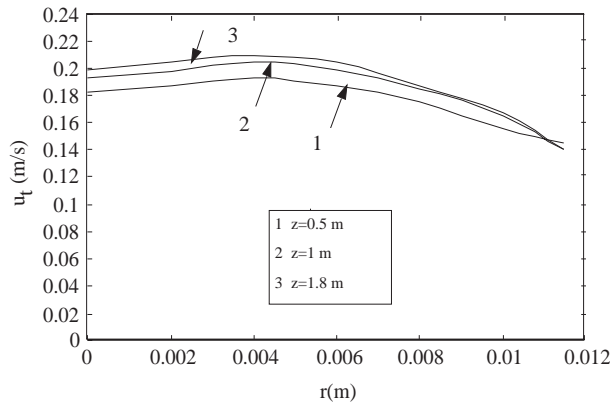


**Figure 4.** Estimated radial temperature profile at three axial locations (case 1).

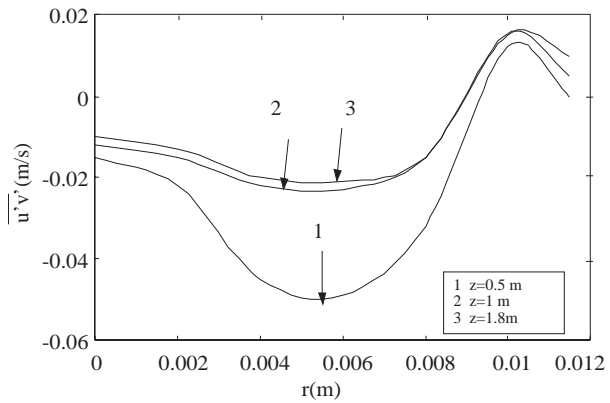
It is seen that liquid velocity increases along the pipe. This is the result of increased steam fraction as boiling occurs and lower density of the steam with respect to the continuous phase (water). The estimated results are compared with those obtained by Lai and Farouk (1993) at  $z=1.8$  m. While the numerical results of Lai and Farouk (1993) exhibit a parabolic velocity distribution where the velocity is maximum at the center and minimum at the vicinity of the wall, the present model predicts maximum liquid velocity at the vicinity of the wall where the void fraction is higher. Recent experimental findings of Roy *et al.* (1997) support the predicted trend in the liquid velocity.

Figure 7 shows the radial turbulence intensity profile in the pipe. The turbulence intensity is calculated as  $u_t = \left(\frac{2}{3}k\right)^{0.5}$  which is the average fluctuation two directions. Turbulence intensity increases

as the void fraction increases. However, this increase is not proportional to the increase in the void fraction. This phenomenon was also observed in an experimental study by Seriwaza *et al.* (1975). The decrease in the turbulence production at the high void fraction may be attributed to energy dissipation associated with the lateral relative motion of the bubbles. The radial distribution of the Reynolds shear stress ( $u'v'$ ) is shown in Fig. 8. It is seen that the magnitude of the shear stress increases in the bubbly region with the void fraction. However, a decrease is obtained after this region; this may be attributed to a more flat velocity distribution as the void fraction increases.



**Figure 7.** Radial turbulence energy distribution at three axial locations



**Figure 8.** Radial Reynolds stress distribution at three axial locations

Figure 9 shows radial void fractions at two locations. It is also seen that at  $z=0.5$  m there are bubbles only very close to the wall while the void fraction at the center increases at a higher location

( $z=1.5$  m). The estimated results were also compared with numerical data of Lai and Farouk (1993). The present study agrees very well with that of Lai and Farouk (1993) at  $z=0.5$  m, while the present study gives a better void fraction profile at  $z=1.5$  m, which agrees with previous experimental observations (Levy, 1967; Pierre and Bankoff, 1967).

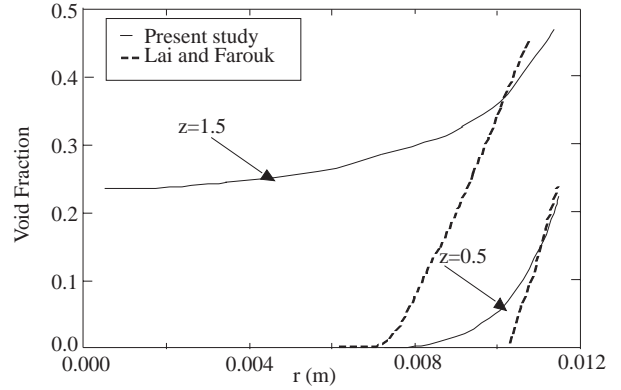


**Figure 9.** Comparison of estimated radial void fraction with that of Lai and Farouk (1993).

The estimated axial void fraction distribution is compared with the experimental data of Bertolemei and Chanturiya (1967) and the numerical data of Lai and Farouk (1993) in Fig. 10. It is seen that the present study and the data of Bertolemei and Chanturiya (1967) and Lai and Farouk (1993) are in very good agreement at high void fractions; however, Lai and Farouk's study slightly underestimated the void distribution at low void fractions and the onset of boiling. Specifically, the present study predicts the initial point of net vapor generation where the void fraction increases rapidly with the heated length better than did Lai and Farouk's study. Figures 11 and 12 compare the present results and those of Bartolemei and Chanturiya (1967) and the numerical result of Lai and Farouk (1993) for the flow conditions summarized in case 2 and 3. It is seen that similar to Fig. 10, again the present results and Lai and Farouk's (1993) data are in agreement with experiment, while present results estimate the initial point of vapor generation better in both cases. Similar results are obtained for the remaining cases given in Table 2. Therefore, they are not presented here for reasons of brevity.

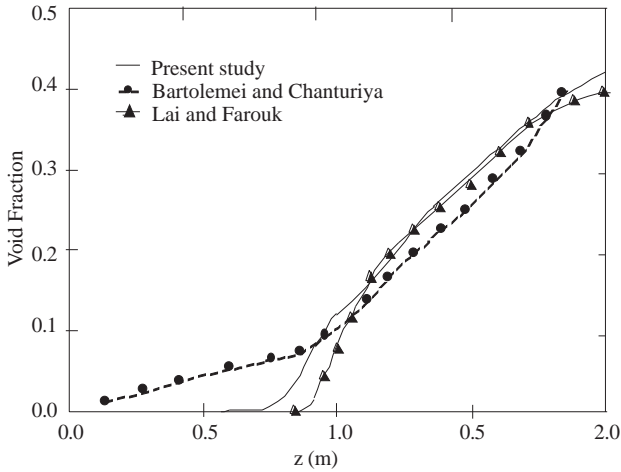


Figure 10. Comparison of estimated axial void fraction (case 1).

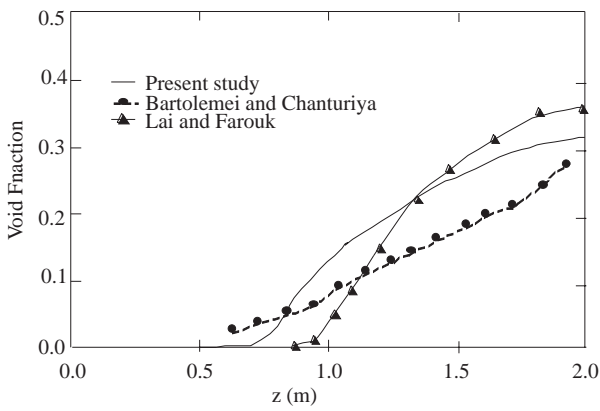


Figure 11. Comparison of estimated axial void fraction (case 2).

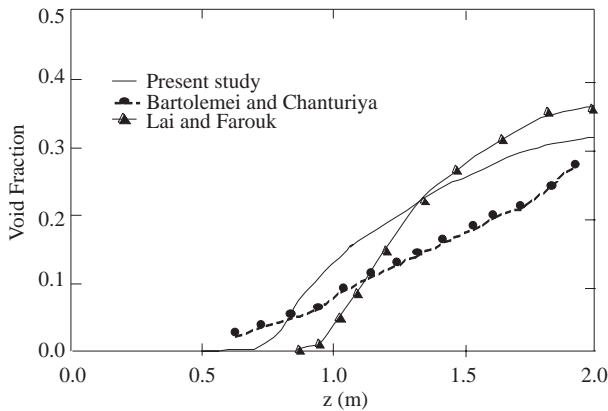


Figure 12. Comparison of estimated axial void fraction (case 3).

### Conclusions

The void fraction profile, temperature distribution and velocity fields for a subcooled boiling of water in a vertical pipe are calculated using a two-fluid model. This model involves solutions of transport equations for the variables of each phase with allowance for interphase transfer of momentum and energy. A modified  $k - \epsilon$  turbulence model is adapted to estimate the turbulence characteristics of the flow. The turbulence model considers the turbulence production due to bubble motion. The estimated results are compared with experimental and numerical data in the literature.

It is found that subcooled water enters the pipe and subsequently boils due to the uniform heating from the pipe wall. Bubbles form adjacent to the heated wall and then move towards the center. The liquid velocity is found to increase along the pipe as the void fraction increases. The maximum liquid velocity occurs near the heated wall.

The estimated void fraction profile agrees satisfactorily with those in the literature. It is found that the present study improves on the results of a previous numerical effort, especially at a lower void fraction. Specifically, the onset of boiling and void distribution are estimated better in this study.

### Nomenclature

- $A_{int}$  interfacial area for unit volume,  $m^2$
- $c_d$  drag coefficient
- $d_b$  bubble diameter,  $m$
- $F$  volumetric inter-fluid friction,  $kg/m^3sn$
- $F_b$  buoyancy forces,  $kg/m^2s^2$
- $g$  gravity vector,  $m/s^2$
- $\dot{G}_k$  production of turbulence energy
- $h$  enthalpy,  $kJ/kg$
- $k$  turbulence energy,  $m^2/s^2$
- $p$  static pressure,  $pa$
- $r$  radial coordinate
- $r_o$  radius
- $Pr$  Prandtl number
- $Re$  Reynolds number
- $T$  temperature,  $^{\circ}C, ^{\circ}K$
- $u$  velocity vector,  $m/s$
- $u_r$  slip velocity,  $m/s$
- $v$  radial velocity component,  $m/s$
- $We$  Weber number
- $w$  axial velocity component,  $m/s$
- $\Delta H$  latent heat of vaporization,  $kJ/kg$



$y^+$  dimensionless distance  
 $z$  axial coordinate

### Greek Letters

$\alpha$  volume fraction  
 $\rho$  density,  $\text{kg/m}^3$   
 $\sigma$  Schmidt number  
 $\varepsilon$  rate of dissipation of turbulent energy,  $\text{m}^2/\text{s}^3$   
 $\gamma$  interfacial tension,  $\text{kg/s}^2$   
 $\kappa$  Von Karman constant  
 $\mu$  viscosity,  $\text{Ns/m}^2$   
 $\tau$  shear stress,  $\text{N/m}^2$   
 $\lambda$  heat transfer coefficient,  $\text{W/m}^2 \text{ }^\circ\text{C}$

### Subscripts

b bubble  
 eff effective  
 G gas phase  
 i gas or Liquid phase  
 int interphase  
 j gas or liquid phase  
 l laminar  
 L liquid phase  
 sat saturation  
 t turbulent

### References

- Bartolemei, G.G., and Chanturiya, V.M., "Experimental Study of True Void Fraction When Boiling Subcooled Water in Vertical Tubes", *Thermal Engineering*, 14, 123-128, 1967.
- Hu, L.W., and Pan, C., "Prediction of Void Fraction in Convective Subcooled Boiling Channels Using a One-Dimensional Two-Fluid Model", *Journal of Heat Transfer*, 117, 799-803, 1995.
- Kroeger, P.G., and Zuber, N., "An Analysis of the Effects of Various Parameters on the Average Void Fractions in Subcooled Boiling", *International Journal of Heat and Mass Transfer*, 11, 211-233, 1968.
- Kuo, J.T., and Wallis, G.B., "Flow of Bubbles Through Nozzles", *International Journal of Multiphase Flow*, 14, 547-556, 1988.
- Lai, J.C. and Farouk, B., "Numerical Simulation of Subcooled Boiling and Heat Transfer in a Vertical Ducts", *International Journal of Heat and Mass Transfer*, 36, 1541-1551, 1993.
- Lance, M., and Bataille, J., "Turbulence in the Liquid Phase of a Uniform Bubbly Air-Water Flow", *Journal of Fluid Mechanics*, 22, 95-118, 1991.
- Launder, B.E., and Spalding, D.B., "The Numerical Computation of Turbulent Flows", *Computational Methods in Applied Mechanics & Engineering*, 3, 269-289, 1974.
- Levy, S., "Forced Convection Subcooled Boiling-Prediction of Vapor Volumetric Fraction", *International Journal of Heat and Mass Transfer*, 10, 951-965, 1967.
- Lopez de Bertodano, M., Lee, S.J., Lahey, R.T., and Drew, D.A., "The Prediction of 2-Phase Turbulence and Phase Distribution Phenomena Using a Reynolds Stress Model", *Journal of Fluids Engineering*, 112, 107-114, 1990.
- Lopez de Bertodano, M., Lahey, R.T., and Jones, O.C., "Phase Distribution in Bubbly Two Phase Flow in Vertical Ducts", *International Journal of Multiphase Flow*, 20, 805-818, 1994.
- Pierre, C.C. St., and Bankoff, S.G., "Vapor Volume Profiles in Developing Two-Phase Flow", *International Journal of Heat and Mass Transfer*, 10, 237-249, 1967.
- Rosten, H., and Spalding, D.B., "Phoenix Manual, CHAM, TR/100", London, 1986.
- Roy, R.P., Velidandla, V., and Kalra, S.P., "Velocity Field in Turbulent Subcooled Boiling Flow", *Journal of Heat Transfer*, 119, 754-766, 1997.
- Serizawa, A., Kataoka, I., and Michiyoshi, I., "Phase Distribution in Bubbly Flow", *Data Set No.24, Proceedings of the Second International Workshop on Two-Phase Flow Fundamentals*, 1986.
- Serizawa, A., Kataoka, I., and Michiyoshi, I., "Turbulence Structure of Air-Water Bubbly Flow-II. Local Properties", *International Journal of Multiphase Flow*, 2, 235-246, 1975.
- Singhal, A.K., and Spalding, D.B., "Mathematical Modeling of Multi-Phase Flow and Heat Transfer in Steam Generators", *2<sup>nd</sup> Multi-Phase Flow and Heat Transfer Symposium Workshop organized by the Clean Energy Research Institute, University of Florida, at Miami Beach, Florida, April 16-18, 1979.*
- Theofanous, T.G., and Sullivan, J.P., "Turbulence in Two-Phase Dispersed Flows", *J. Fluid Mech.*, 116, 343-362, 1982.
- Wang, S.K., Lee, S.J., Jones, O.C., and Lahey, R.T., "3-D Turbulence Structure and Phase Distribution Measurements in Bubbly Two-Phase Flows", *International Journal of Multiphase Flow*, 13, 327-343, 1987.

Zeitoun, O., and Shoukri, M., "Axial Void Fraction Profile in Low Pressure Subcooled Flow Boiling", *International Journal of Heat and Mass Transfer*, 40, 869-879, 1997.

Zuber, N., Staub, F.W., and Bijwaard, G., "Vapor Void Fraction in Subcooled Boiling and in Saturated

Boiling Systems", *Proceeding of the Third International Heat Transfer Conference*, Chicago, 5, 24-35, 1966.

Zuber, N. and Findlay, J., "Average Volumetric Concentration in Two-Phase Flow Systems", *Journal of Heat Transfer*, 87C, 453-462, 1965.